Article:
Zhang, Z-Q and Yang, G-Z (2014) Calibration of miniature inertial and magnetic sensor units for robust attitude estimation. IEEE Transactions on Instrumentation and Measurement, 63 (3). pp. 711-718. ISSN: 0018-9456

https://doi.org/10.1109/TIM.2013.2281562

Calibration of Miniature Inertial and Magnetic Sensor Units for Robust Attitude Estimation

Zhi-Qiang Zhang and Guang-Zhong Yang, *Fellow, IEEE*

***Abstract*—Attitude estimation from miniature inertial and magnetic sensors has been used in a wide variety of applications, ranging from virtual reality, underwater vehicles, handheld navigation devices, to biomotion analysis. However, appropriate sensor calibrations for accurate sensor measurements are essential to the performance of attitude estimation algorithms. In this paper, we present a robust sensor calibration method for accurate attitude estimation from 3-axis accelerometers, gyroscopes and magnetometer measurements. The proposed calibration method only requires a simple pan-tilt unit. A unified sensor model for inertial and magnetic sensors is used to convert the sensor readings to physical quantities in metric units. Based on the sensor model, a cost function is constructed, and a two-step iterative algorithm is then proposed to calibrate the inertial sensors. Due to the difficulties of acquiring the ground-truth of the Earth magnetic field, a simplified pseudo-magnetometer calibration method is also presented based on an ellipsoid fitting algorithm. The calibration method is then applied to our sensor nodes, and the good performance of the orientation estimation has illustrated the effectiveness of the proposed sensor calibration method.**

***Index Terms*—Miniature Sensors, Calibration, Orientation/Attitude, Kalman Filter, Optimization**

I. Introduction

With continuing development of micro-electro-mechanical system (MEMS) technology, micro-inertial/magnetic sensors have been widely used to acquire attitude information for a wide variety of applications [1]. Extensive research has been performed on how to fuse inertial/magnetic sensor measurements for accurate attitude estimation. For example, Yun et al. [2] presented the design of an extended Kalman filter to estimate the orientation of human limbs using a combination of inertial sensors and magnetic sensors. We also had the similar work [3] [4]. Robertson et al. [5] and Floor-Westerdijk et al. [6] further extended the orientation estimation using inertial sensors, and they proposed to estimate the sensor displacement as well in pedestrian self-navigation. However, the achievable accuracy is highly dependent on the quality of the inertial/magnetic sensor measurements. In general, the main sources of sensor error include bias, scale factor and misalignment; therefore, appropriate sensor calibration is critical to the accuracy and overall system performance.

Thus far, most existing inertial/magnetic sensor calibration methods rely on additional instruments, such as mechanical platforms or optical tracking devices. By turning the sensor unit in different orientations with known turn rates, the sensor model parameters can be estimated from the sensor output and pre-calculated acceleration, magnetic field and turn rates [7] [8] [9]. Unfortunately, these mechanical platforms and optical tracking systems tend to be expensive and impractical for routine applications. For this reason, alternative methods that do not require these additional platforms have been pursued. To this end, Marioli et al. [10] and Lötters et al. [11] applied the gravity vector twice to each axis of the accelerometer to estimate the offset and scale factors by relying on the fact that the modulus of the acceleration vector measured by a triaxial accelerometer should be g. Wu et al. [12] constructed a nonlinear function to describe the relationship between gravity and sensor parameters. A Taylor expansion was used to linearize the nonlinear function and linear unbiased estimators with minimum variance were used as the offset and gain. However, the main disadvantage of these methods is that they ignored the misalignment error. Skog et al. [13] further extended their work by incorporating misalignment errors for inertial sensor calibration. A cost function was first constructed and then minimized with respect to the unknown sensor model parameters using Newton-Raphson method. Syed et al. [14], Shen et al. [15] and Li et al. [16] also presented similar work for accelerometer and gyroscope calibration. Although some improvements have been achieved, they are still susceptible to misalignment errors. Due to the difficulties of acquiring the ground-truth of the magnetic field, the above mentioned inertial sensor calibration methods are not applicable to the magnetometer calibration. For this reason, a number of solutions based on the ellipsoid fitting have been proposed to calibrate erroneous magnetometers. For instance, Gebre-Egziabher et al. [17] attempted to find an ellipsoid which best fit the measured magnetometer data based on a simplified sensor error model. Renaudin et al. [18] further improved the error model and presented an adaptive least squares estimator which provided a consistent solution to the ellipsoid fitting problem. Similarly, Vasconcelos et al. [19] proposed an iterative Maximum Likelihood Estimator (MLE) to fit the sensor measurements to an ellipsoid manifold. A separate closed-form optimal algorithm was then presented to estimate the misalignment matrix. Unfortunately, all these methods still require some magnetic field information in advance.

The motivation of this paper is to tackle the misalignment problem for inertial sensor calibration using a simple pan-tilt unit. It aims to provide an accurate attitude estimation scheme from micro inertial/magnetic sensors based on minimum-order linear Kalman filers [20]. In our method, a unified sensor model is presented to convert sensor readings to physical quantities in metric units. Based on the sensor model, a cost function is constructed, and a two-step iterative algorithm is

The authors are with the Hamlyn Centre for Robotic Surgery, Imperial College London, SW7 2AZ London, U. K. (e-mail: z.zhang@imperial.ac.uk).

then proposed to calibrate the inertial sensors. Due to the difficulties of acquiring the ground-truth of the Earth magnetic field, a simplified pseudo-magnetometer calibration is also presented based on the ellipsoid fitting method. To demonstrate the practical value of the proposed technique, detailed laboratory experiments with known ground-truth measurements have been performed. The derived results demonstrate that the proposed method can provide accurate orientation estimation after the sensor calibration.

The rest of the paper is organized as follows. The proposed sensor calibration procedures, including the unified sensor model, the two-step iterative method, and the ellipsoid fitting method are elaborated in section II. Experimental results and conclusions are provided in sections IV and V of the paper, respectively.

II. Our method

A. Unified sensor model

For the description of the MEMS sensors, all sensor readings need to be converted to physical quantities in metric units. Meanwhile, the three sensor sensitivity axes should ideally be orthogonal to each other, and the triad constructed by the three axes must be aligned to a reference coordinate system. In practice, this is difficult to achieve. A unified triaxial sensor model is therefore used, with which all these issues are considered.

Mathematically, the triaxial sensor model can be written in a vector form, where index k represents the sensor type (i.e., *a, g* or *m* for accelerometer, gyroscope or magnetometer respectively). Due to inevitable sensor errors, the three sensitivity axes are not always orthogonal to each other, so orthogonalization of the axes is necessary. Denote T_k as the Gram-Schmidt orthogonalization matrix, so T_k can be written as:

$$T_k = \begin{bmatrix} 1 & 0 & 0 \\ \alpha_k & 1 & 0 \\ \beta_k & \gamma_k & 1 \end{bmatrix}. \tag{1}$$

As shown in Fig. 1, the new sensor sensitivity axes may not be aligned to the reference coordinates perfectly after Gram-Schmidt orthogonalization, so the rotation matrix R transforming the sensor reading in orthogonal sensitivity axes to the reference coordinates can be written as :

$$R_k = R_Z(\psi)R_Y(\theta)R_X(\phi) \tag{2}$$

where

$$R_X(\phi) = \begin{bmatrix} 1 & 0 & 0 \\ 0 & cos(\phi) & -sin(\phi) \\ 0 & sin(\phi) & cos(\phi) \end{bmatrix}, \tag{3}$$

$$R_Y(\theta) = \begin{bmatrix} cos(\theta) & 0 & sin(\theta) \\ 0 & 1 & 0 \\ -sin(\theta) & 0 & cos(\theta) \end{bmatrix} \tag{4}$$

and

$$R_Z(\psi) = \begin{bmatrix} cos(\psi) & -sin(\psi) & 0 \\ sin(\psi) & cos(\psi) & 0 \\ 0 & 0 & 1 \end{bmatrix}. \tag{5}$$

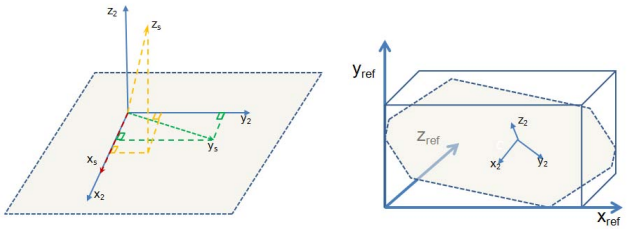

(a) (b)

Figure 1. Schematic illustration of sensor misalignment. (a) The nonorthogonal axes x_s, y_s and z_s can be aligned to the orthogonal axes x_2, y_2 and z_2. (b) The x_2, y_2 and z_2 can then be aligned to a reference system x_{ref}, y_{ref} and z_{ref}.

Before orthogonalization and coordinates alignment, the output of the MEMS sensors should be converted to physical quantities in metric units. The typical relationship between the output and physical quantities can be described by a linear equation, typically given in the manufactures data sheet, but the exact linear equation parameters (scale factors and bias) for each sensor can have minor variations. Define the scale factor matrix

$$S_k = \begin{bmatrix} s_{kx} & 0 & 0 \\ 0 & s_{ky} & 0 \\ 0 & 0 & s_{kz} \end{bmatrix}$$

and bias vector $b_k = [b_{kx},\ b_{ky},\ b_{kz}]^T$, the sensor unified model can be written as:

$$u_k = R_k T_k S_k (y_k - b_k), \tag{6}$$

where u_k is the measured physical quantities in metric unit, and the y_k is sensor voltage readings.

B. Inertial Sensor Calibration

The purpose of the sensor calibration is to estimate the value of parameter vector

$$\zeta = [\alpha_k, \beta_k, \gamma_k, \phi, \psi, \theta, s_{kx}, s_{kx}, s_{kx}, b_{kx}, b_{ky}, b_{kz}]^T \tag{7}$$

given J pairs of physical quantities u_k^j and the corresponding y_k^j, where $j = 1, 2, \cdots, J$. The estimation of ζ can be written as:

$$\hat{\zeta} = \underset{\zeta}{\operatorname{argmin}}\{L(\zeta)\} \tag{8}$$

where

$$L(\zeta) = \sum_{j=1}^{J} \left\| u_k^j - R_k T_k S_k (y_k^j - b_k) \right\|^2. \tag{9}$$

and $\|\cdot\|$ is the Frobenius norm. Here, j is the index of different orientation or rotation that the pan-tilt calibration unit is set to. Due to the nonlinearity of (9), it is difficult to find a globally optimized solution for ζ in practice. In this paper, we propose a two-step parameter estimation scheme to ease the optimization process, i.e., 1) the sensor bias b_k is estimated separately; 2) Unlike Bonnet. et al [21] estimating the other 9 parameters $(\alpha_k, \beta_k, \gamma_k, \phi, \psi, \theta, s_{kx}, s_{kx}, s_{kx})$ individually,

we estimate matrix $H_k = R_k T_k S_k$ instead, which can also take the other unmodelled linear time invariant errors and distortions into account.

1) Accelerometer Calibration:

Lemma 1: Denote: $Y_a = \left(y_a^1, y_a^2 \cdots, y_a^J\right)$ as the sensor reading matrix, $U_a = \left(u_a^1, u_a^2 \cdots, u_a^J\right)^T$ as the corresponding physical quantity matrix, and $B_a = \mathbb{R}(b_a)$ as the bias matrix which has J columns and each column is set to b_a. Given an initial value $b_{a,0}$, the H_a and b_a can be estimated as:

1. Set index i=1;
2. Constructing the bias matrix $B_{a,i-1}$ as:
$$B_{a,i-1} = \mathbb{R}(b_{a,i-1}) \tag{10}$$
3. Calculate $H_{a,i}$ as:
$$H_{a,i} = U_a \cdot (Y_a - B_{a,i-1})^+ \tag{11}$$
where $(Y_a - B_{a,i-1})^+$ is the pseudoinverse of Y_a–$B_{a,i-1}$.
4. Calculate $b_{a,i}$ as
$$\begin{aligned} b_{a,i} =& \mathbb{E}(Y_a - H_{a,i}^+ \cdot U) \\ =& \frac{\sum_{j=1}^{J}\left(y_a^j - \left(H_{a,i}^+ \cdot U\right)_{(j)}\right)}{J} \end{aligned} \tag{12}$$
where $\mathbb{E}(\cdot)$ is the mean value operator, and $\left(H_{a,i}^+ \cdot U\right)_{(j)}$ is the jth column of matrix $\left(H_{a,i}^+ \cdot U\right)$.
5. set $i = i + 1$ and repeat steps $2 - 5$ until H_a and b_a converge.

The purpose of the accelerometer calibration is to minimize

$$\left\| U_a - H_a(Y_a - B_a) \right\|. \tag{13}$$

To make sure H_a and b_a converge, we need to prove in each iteration that:

$$\left\| U_a - H_{a,i}(Y_a - B_{a,i-1}) \right\| \leqslant \left\| U_a - H_{a,i-1}(Y_a - B_{a,i-1}) \right\| \tag{14}$$

and

$$\left\| U_a - H_{a,i}(Y_a - B_{a,i}) \right\| \leqslant \left\| U_a - H_{a,i}(Y_a - B_{a,i-1}) \right\|. \tag{15}$$

The proofs for equation (14) and (15) are give in the Appendix at the end of this paper.

2) Gyroscope Calibration: Similar to accelerometer calibration, we also estimate the gyroscope bias b_g and transformation matrix H_g separately. Unlike the accelerometer calibration process, no iteration is required for gyroscope calibration as the bias b_g can be estimated accurately. For this reason, the gyroscope calibration mainly consists of two steps:

1. The sensor node is placed at J_1 different orientations and remain stationary, which means that $u_g^j = 0, j = 1, 2 \cdots, J_1$. Denote $U_g = \left(u_g^1, u_g^2 \cdots, u_g^{J_1}\right)^T = 0$, and the corresponding gyroscope readings as $Y_g = \left(y_g^1, y_g^2 \cdots, y_g^{J_1}\right)$, and the gyroscope bias $B_g = \mathbb{R}(b_g)$, we can then get:
$$H_g \cdot (Y_g - B_g) = U_g = 0 \tag{16}$$
As $det(H_g) = det(R_g)det(T_g)det(S_g) \neq 0$ (here det means determinant), so H_g is a full rank matrix. We should have
$$Y_g - B_g = 0. \tag{17}$$
By taking sensor noise into account, we set bias b_g as the mean value:
$$b_g = \frac{\sum_{j=1}^{J_1} y_g^j}{J_1}. \tag{18}$$
2. Rotate the sensor node using the pan-tilt unit at $J_2 = J - J_1$ different angular rates $U_g = \left(u_g^1, u_g^2 \cdots, u_g^{J_2}\right)^T$. Denote the corresponding gyroscope output as $Y_g = \left(y_g^1, y_g^2 \cdots, y_g^{J_2}\right)$, we can get H_g as
$$H_g = U_g \cdot (Y_g - \mathbb{R}(b_g))^+ \tag{19}$$
For simplicity, we still used symbols Y_g and U_g to represent the new sensor output and angular rate.

C. Pseudo-Magnetometer Calibration

Similar to accelerometer calibration, we define: $Y_m = \left(y_m^1, y_m^2 \cdots, y_m^J\right)$ as the sensor reading matrix,$U_m = \left(u_m^1, u_m^2 \cdots, u_m^J\right)^T$ as the corresponding matrix for physical quantities. However, it is difficult to acquire magnetic quantities u_m^j without a complex platform, but the norm of the magnetometer vector measurement u_m^j should be equal to the magnitude of the Earth magnetic field in a perturbation-free environment. Denote the magnitude of the Earth magnetic field as M, we have

$$\| H_m \cdot \left(y_m^j - b_m\right) \| = \| u_m^j \|. \tag{20}$$

By expanding the above equation, we can get:

$$\left(y_m^j - b_m\right)^T \cdot (H_m)^T \cdot H_m \cdot \left(y_m^j - b_m\right) = M^2. \tag{21}$$

As the Earth magnetic field itself is spatially varying, it is difficult to get the exact value of M. In this paper, the magnitude M is normalized. Another advantage of the normalization process is that the precondition of perturbation free-environment is no longer necessary. When the magnetometer is calibrated, perturbation is permitted as long as it is constant. The above equation can then be written as:

$$\left(y_m^j - b_m\right)^T \cdot \left(\frac{H_m}{M}\right)^T \cdot \frac{H_m}{M} \cdot \left(y_m^j - b_m\right) = 1. \tag{22}$$

This equation represents an arbitrarily oriented ellipsoid, centered at b_m. Meanwhile, the eigenvectors of the inverse matrix of $\left(\left(\frac{H_m}{M}\right)^T \cdot \frac{H_m}{M}\right)$ define the principal directions of the ellipsoid and the square root of the eigenvalues are the corresponding equatorial radii.

The magnetometer calibration problem now becomes finding an arbitrarily oriented ellipsoid which fits the J points $y_m^1, y_m^2 \cdots, y_m^J$ best. There is abundant literature addressing this problem [22] [23] [24]. For this study, the least squares ellipsoid fitting method proposed in [25] is used. We can derive ellipsoid center v_c, the eigenvectors v_e^1, v_e^2, v_e^3 for the inverse matrix of $\left(\left(\frac{H_m}{M}\right)^T \cdot \frac{H_m}{M}\right)$ and the equatorial radii r_1, r_2, r_3. Therefore, we have

$$b_m = v_c \tag{23}$$

and

$$\left(\left(\frac{H_m}{M}\right)^T \cdot \frac{H_m}{M}\right)^+ = \left(r_1^2 v_e^1, r_2^2 v_e^2, r_3^2 v_e^3\right)\left(v_e^1, v_e^2, v_e^3\right)^+, \tag{24}$$

so

$$\left((H_m)^T \cdot H_m\right) = M^2 Q, \tag{25}$$

where $Q = \left(\left(r_1^2 v_e^1, r_2^2 v_e^2, r_3^2 v_e^3\right)\left(v_e^1, v_e^2, v_e^3\right)^+\right)^+$. As Q is a positive definite matrix, an eigen-decomposition can be applied:

$$Q = \Lambda D \Lambda^T \tag{26}$$

where Λ corresponds to the eigenvectors of Q, and D is the diagonal matrix containing the eigenvalues, so we can define another Matrix B as

$$B = M\Lambda\sqrt{D}\Lambda^T \tag{27}$$

and B satisfies

$$\begin{aligned} B^T B =& M\Lambda\sqrt{D}\Lambda^T M S\sqrt{D}\Lambda^T \\ =& M^2 \Lambda D \Lambda^T \\ =& M^2 Q. \end{aligned} \tag{28}$$

Given any rotational matrix Ω, we can have

$$\begin{aligned} (\Omega B)^T \Omega B =& M S\sqrt{D}\Lambda^T \Omega^T \Omega M \Lambda\sqrt{D}\Lambda^T \\ =& M^2 \Lambda D \Lambda^T \\ =& M^2 Q. \end{aligned} \tag{29}$$

The above equation illustrates that H_m can be any matrix in the form of ΩB, so it is impossible to acquire the exact magnetometer parameter H_m, while b_m can estimated accurately; therefore, we empirically set H_m according to the magnetometer datasheet for orientation estimation.

III. Experimental and Simulation Results

In order to evaluate the performance of the proposed sensor calibration method, detailed simulation and laboratory experiments were conducted. For the simulation study, we selected Monte Carlo simulation to illustrate the performance of the sensor calibration method. For the results presented in this paper, we used the Body Sensor Network (BSN) platform [26] developed by our lab, which consists of three stackable daughter boards: the sensor board, the main processor board, and the battery board. They are connected via a stackable connector design as shown in Fig. 2(a). Each BSN node used is equipped with an Analog Devices ADXL330 [27] for 3D acceleration measurement, an InvenSense ITG-3200 digital gyroscope [28] for 3D angular velocity measurement, and a Honeywell HMC5843 [29] for 3D magnetic field measurement. In order to calibrate the BSN node, a bespoke housing for the BSN node is designed as shown in Fig. 2(b). The unique feature of the box is that all six sides of the box feature the same mounting mechanism. After applying the sensor calibration method to our BSN node, we then used the node for attitude estimation, and compared the estimated attitude to reference measurements by the BTS SMART-D optical motion tracking system [30]. The BTS system used in our experiment consisted of 9 cameras installed on the ceiling as shown in Fig. 3. By capturing the positions of the 3 reflective markers on the rigid body that the BSN housing is attached to, an error less than 0.267mm on a volume of $2.95 \times 1.65 \times 3.08m$ was achieved by the BTS system.

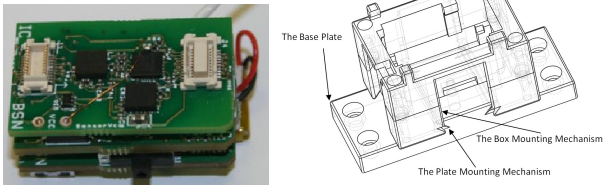

(a) (b)

Figure 2. The BSN hardware platform used for this study. (a) BSN Sensor Node and its stackable sensor daughter boards. (b) The bespoke housing for the BSN Sensor Node.

Figure 3. The BTS SMART-D system used for this study and the BSN node mounted with reflective markers for orientation accuracy evaluation.

A. Sensor Calibration Performance Evaluation

In this step of the evaluation process, as the calibration procedures of the accelerometer and gyroscope are similar, we only present the simulation results for the accelerometer here. In the simulation, the estimation of the accelerometer sensor model parameters were studied when the sensor node was rotated into randomly selected 20 different orientations. However, a zero mean Gaussian distributed error with variance $0.01m/s^2$ was added to the measured physical quantities u_a to reflect sensor noise. In Table I, the settings used in the simulation are summarized.

Table I
Model parameters used for accelerometer calibration

Misalignment.	Rotation	Scaling (m/s^2)	Base
$\alpha_a = 0.1$	$\phi_a = 0.1$	$s_{ax} = 9.8/467$	$b_{ax} = 2429$
$\beta_a = 0.1$	$\theta_a = 0.1$	$s_{ay} = 9.8/412$	$b_{ay} = 2318$
$\gamma_a = 0.1$	$\psi_a = 0.1$	$s_{az} = 9.8/438$	$b_{az} = 2368$

After setting the parameters, the true value for H_a and b_a are

$$H_a = \begin{bmatrix} 0.0207759 & 0.0002280 & 0.0044495 \\ 0.0020845 & 0.0238093 & 0.0004390 \\ -0.0020950 & 0.0021253 & 0.0221503 \end{bmatrix}$$

and $b_a = (2429, 2318, 2368)^T$. The simulation results for b_a and H_a are given in Fig. 4 and Fig. 5 respectively. The estimation results by the optimization method [13] are also presented for comparison. As we can see from the figures, it is evident that:

- The iterative parameter estimation method is relatively fast to converge. After 6 iterations, the estimations for b_a and H_a are close to their respective ground-truth values.
- More specifically, the estimation of b_a is $(2428.0, 2318.3, 2367.7)^T$ after 6 iterations, while b_a converges to $(2428.9, 2318.0, 2367.9)^T$ after 10 iterations. The error between b_a true value and estimated value is less than 0.1, which demonstrates the effectiveness of the proposed method for inertial sensor bias parameter estimation. The optimization method can also converge to the ground-truth of the bias, but with much slower convergence.
- Meanwhile, H_a also converges to

$$\begin{bmatrix} 0.0207788 & 0.0002256 & 0.0044509 \\ 0.0020850 & 0.0238117 & 0.0004396 \\ -0.0020943 & 0.0021244 & 0.0221500 \end{bmatrix}$$

after 10 iterations. Comparing this matrix to the ground-truth of H_a, the error is less than 0.015%, which is negligible. As we have mentioned earlier, the optimization method is not able to estimate the misalignment error, which caused the non-convergence of H_a estimation.

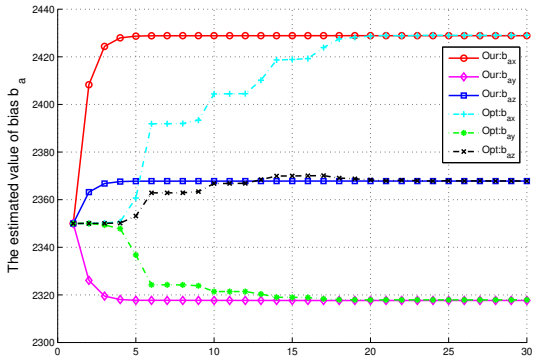

Figure 4. Estimation results for b_a, showing that the estimation value converges after 6 iterations using the proposed method and the optimization method proposed in [13].

Table II
ITERATIVE RESULTS OVER 100 SIMULATIONS (SHOWN AS MEAN±STD)

	b_{ax}	b_{ay}	b_{az}	$\|H_a - \hat{H}_a\| \times 10^3$
Iteration 2	2398.2±0.74	2330.5±0.69	2360.9±0.91	2.09±0.005
Iteration 5	2426.9±1.20	2318.8±1.09	2367.4±1.44	0.32±0.006
Iteration 10	2429.0±1.24	2318.0±1.12	2367.9±1.48	0.02±0.005
Iteration 20	2429.0±1.24	2318.0±1.12	2367.9±1.48	0.02±0.005

The simulation was repeated for another 100 times, and statistical results for b_a and H_a are given in Table II. It can be seen that the proposed iterative method converges after 10 iterations with negligible errors ($< 0.07\%$). In conclusion, the above analysis has shown that the proposed accelerometer calibration method can estimate the accelerometer sensor model parameters accurately.

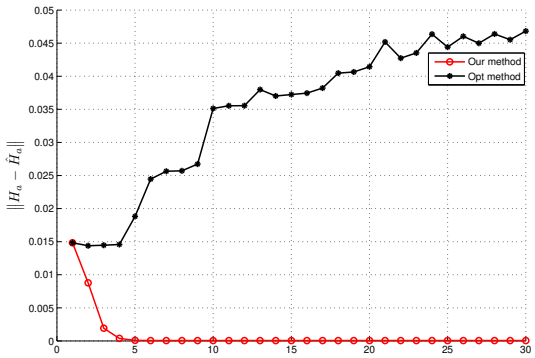

Figure 5. Estimation results for matrix H_a, showing that after 6 iterations, the Frobenius norm $\|H_a - \hat{H}_a\|$ converges to 0, i.e., $H_a = \hat{H}_a$.

For the second simulation, we evaluated the magnetometer sensor model parameters estimated when we randomly put the sensor at 20 different orientations. A zero mean Gaussian distributed error with variance $0.1mg$ was added to the voltage readings y_m to simulate sensor noise. Table III summarizes the settings used.

The b_m estimation results calculated from 100 simulated calibrations using the proposed magnetometer calibration method are shown in Fig. 6. As we can see from the figure, the mean errors between the estimated b_m and the true b_m are less than 1, and the maximum estimation error is less than 0.049%, which is small and imperceptible. In conclusion, the above analysis has shown that the proposed magnetometer calibration method can estimate the bias values accurately.

It should be noted, however, one limitation of the proposed magnetometer calibration method is that the H_m cannot be determined. In the next part of our evaluation, we will show that the proposed calibration method can still improve the attitude estimation accuracy significantly without the need of knowing the exact value of H_m.

B. The Performance of Attitude Estimation

After applying the calibration method to our sensor nodes, we then fused the sensor measurements for attitude estimation using our previous method [20]. Since it is well known that the inertial sensor cannot sense the absolute rotation about the vertical axis accurately due to inertial drift, magnetometers are used to compensate the inertial sensor and measure the

Table III
MODEL PARAMETERS FOR MAGNETOMETER SENSOR CALIBRATION

Misalignment.	Rotation	Scaling (mg)	Base
$\alpha_m = 0.1$	$\phi_m = 0.1$	$s_{ax} = 1/1300$	$b_{ax} = 32768$
$\beta_m = 0.1$	$\theta_m = 0.1$	$s_{ay} = 1/1380$	$b_{ay} = 32877$
$\gamma_m = 0.1$	$\psi_m = 0.1$	$s_{az} = 1/1320$	$b_{az} = 32908$

orientation relative to the vertical. In order to qualitatively illustrate how the magnetometer calibration affects the orientation estimation, a simple experiment was designed using calibrated inertial sensors. In this experiment, we put the BSN sensor node on a platform and then rotate the sensor node around the vertical axis for about 90°, waited for about 7s and then rotated for another 90°.

In this experiment, we only evaluated the rotated angle of the sensor node, which is shown in Fig. 7. In general, the sensor node attitude information and the rotated angle should be constant when the sensor node is stationary. In our experiment, the BSN node was always kept still during the experiment except the two short periods when the sensor node was rotated, so the rotated angle should only change during these short periods. It is evident from the figure that the rotated angle still has noticeable changes after the sensor node is still if the magnetometer is not calibrated. After magnetometer calibration, the rotated angle become accurate and is consistent with the experiment settings and BTS measurements.

To further illustrate the strength of the proposed BSN calibration method, we compare the sensor based attitude estimation result with the reference measurement from the BTS optical motion tracker quantitatively. In our experiment, the BSN sensor node was placed on a rigid body affixed and rotated arbitrarily. Fig. 8 shows the estimated Euler angles by using our proposed method as compared to the ground-truth measurements from the BTS system. It is evident that the proposed sensor calibration can estimate the BSN sensor model parameters accurately, and there are significant estimation errors between the BTS measurements and the estimation before calibration. This is mainly due to the gyroscope suffering from serious integration drift without calibration. Furthermore, the un-calibrated magnetometer cannot compensate for the drift, so the estimated attitude has a significant distortion in the vertical axis. The estimated pitch angle after the optimization calibration [13] also got significant errors, this is mainly due to the inaccurate misalignment estimation during the calibration. The quantitative comparison results between the BTS system and BSN sensor platform are shown in Table IV. From the results derived, it is evident that the proposed method

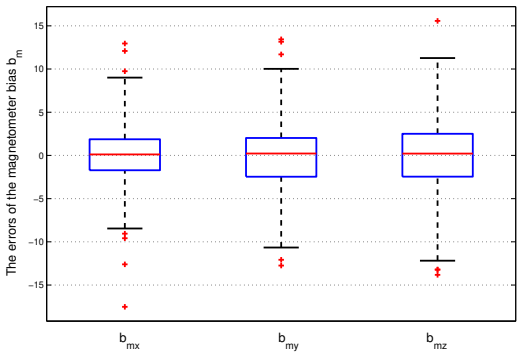

Figure 6. The box-and-whisker error diagram for magnetometer bias estimation, showing the mean error being less than 0.003%, and the maximum error less than 0.049%

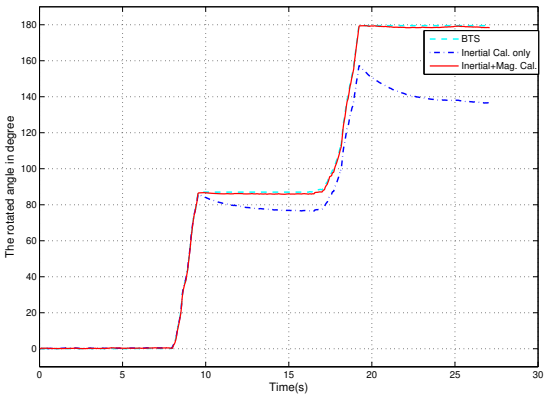

Figure 7. The 90° rotation experiment result showing the improvement in the rotated angle estimation after magnetic calibration.

significantly reduces the root mean square (RMS) errors. There is an excellent correlation between the calibrated result with that of the BTS system.

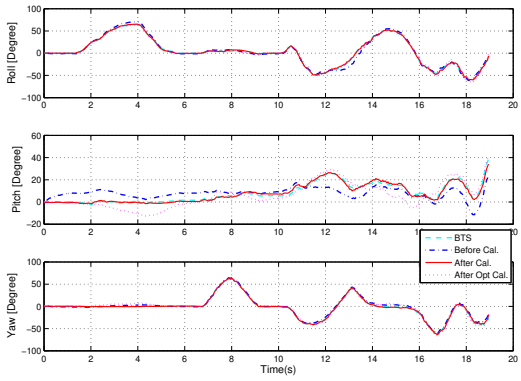

Figure 8. The Euler angle estimation results compared to the BTS measurements after sensor calibration.

Table IV
THE RMS, MEAN, SD AND CORRELATION COEFFICIENTS OF THE ESTIMATED ATTITUDE COMPARED TO THE BTS OPTICAL SYSTEM.

	Optimization Calibration [13]		**Our calibration**	
	RMS (Mean,SD)	Correlation Coefficient	RMS (Mean,SD)	Correlation Coefficient
Roll	0.0380 (0.0035±0.0379)	0.9976	0.0213 (-0.0019±0.0212)	0.9992
Pitch	0.0919 (0.0378±0.0838)	0.9112	0.0240 (0.0028±0.0238)	0.9862
Yaw	0.0557 (-0.0172±0.0530)	0.9921	0.0231 (0.0035±0.0228)	0.9984

The above analyses have shown that the proposed inertial and magnetometer calibration method can significantly improve the attitude estimation accuracy, which suggests that the calibration method can estimate the underlying sensor model parameters accurately. Based on the derived sensor model, the sensor readings can be converted to physical quantities in metric units for accurate attitude estimation.

IV. Conclusion and Future Work

In conclusion, we have presented a method for calibrating micro inertial/magnetic sensors for accurate attitude estimation. A unified sensor model for inertial and magnetic sensors is presented and a novel sensor model parameters estimation method for accelerometer, gyroscope and magnetometer is proposed. The calibration method was applied to the BSN sensor node to acquire accurate acceleration, angular rate and pseudo-magnetic field measurements, which could be fused by a quaternion-based linear Kalman filter to accurately derive the attitude information. The experimental results show that more accurate orientation information can be derived after effective sensor calibration. It is expected that the method can be used for a range of motion estimation applications including robotic navigation and human biomotion analysis.

In this paper, the temperature related sensor drift has not been addressed yet. Therefore, further work is required for continuous self-calibration with consideration of different temporal characteristics of the sensors combined with the use of temperature controlled casing designs to minimise these errors. It is also possible to model and incorporate temperature related drift characteristics as the prior combined with real-time temperature monitoring to cater for these changes. Furthermore, more accurate magnetometer calibration method will also be studied.

Appendix

A. Proof of equation (14)

Proof:

$$\begin{aligned}&\left\|U_a - H_{a,i}(Y_a - B_{a,i-1})\right\| \\ =&\left\|U_a - U_a \cdot (Y_a - B_{a,i-1})^+ (Y_a - B_{a,i-1})\right\| \\ =&\left\|U_a \left(I - (Y_a - B_{a,i-1})^+ (Y_a - B_{a,i-1})\right)\right\|\end{aligned} \tag{30}$$

For any matrices Υ and A, $\left\|I - \Upsilon^+\Upsilon\right\| < \left\|I - A^+\Upsilon\right\|$ is always satisfied unless $\Upsilon = A$, so

$$\begin{aligned}&\left\|U_a - H_{a,i}(Y_a - B_{a,i-1})\right\| \\ \leqslant&\left\|U_a \left(I - (Y_a - B_{a,i-2})^+ (Y_a - B_{a,i-1})\right)\right\| \\ =&\left\|U_a - U_a \cdot (Y_a - B_{a,i-2})^+ (Y_a - B_{a,i-1})\right\| \\ =&\left\|U_a - H_{a,i-1}(Y_a - B_{a,i-1})\right\|\end{aligned} \tag{31}$$

■

B. Proof of equation (15)

Proof:

Denote:

$$\hat{U}_{a,i} = H_{a,i}(Y_a - B_{a,i-1}) \tag{32}$$

we can get:

$$\begin{aligned}b_{a,i} &= \mathbb{E}\left(Y_a - H^+_{a,i} \cdot U_a\right) \\ &= \mathbb{E}\left(Y_a - H^+_{a,i} \cdot \left(\hat{U}_{a,i} + U_a - \hat{U}_{a,i}\right)\right) \\ &= \mathbb{E}\left(Y_a - H^+_{a,i} \cdot \hat{U}_{a,i}\right) - \mathbb{E}\left(H^+_{a,i} \cdot \left(U_a - \hat{U}_{a,i}\right)\right) \\ &= b_{a,i-1} - \mathbb{E}\left(H^+_{a,i} \cdot \left(U_a - \hat{U}_{a,i}\right)\right)\end{aligned} \tag{33}$$

and then,

$$\begin{aligned}&H_{a,i}(Y_a - B_{a,i}) \\ =&H_{a,i}\Big(Y_a - \mathbb{R}\Big(b_{a,i-1} - \mathbb{E}\Big(H^+_{a,i} \cdot \left(U_a - \hat{U}_{a,i}\right)\Big)\Big)\Big) \\ =&H_{a,i}\Big(Y_a - B_{a,i-1} + \mathbb{R}\Big(\mathbb{E}\Big(H^+_{a,i} \cdot \left(U_a - \hat{U}_{a,i}\right)\Big)\Big)\Big) \\ =&\hat{U}_a + H_{a,i}\left(\mathbb{R}\left(\mathbb{E}\left(H^+_{a,i} \cdot \left(U_a - \hat{U}_{a,i}\right)\right)\right)\right) \\ =&\hat{U}_a + \mathbb{R}\left(\mathbb{E}\left(U_a - \hat{U}_{a,i}\right)\right).\end{aligned} \tag{34}$$

We can then get

$$\begin{aligned}&\left\|U_a - H_{a,i}(Y_a - B_{a,i})\right\| \\ =&\left\|U_a - \left(\hat{U}_a + \mathbb{R}\left(\mathbb{E}\left(U_a - \hat{U}_{a,i}\right)\right)\right)\right\| \\ =&\left\|U_a - H_{a,i}(Y_a - B_{a,i-1}) - \mathbb{R}\Big(\mathbb{E}\Big(U_a - \hat{U}_{a,i}\Big)\Big)\right\| \\ \leqslant&\left\|U_a - H_{a,i}(Y_a - B_{a,i-1})\right\|\end{aligned} \tag{35}$$

■

Acknowledgment

The authors would like to thank Dr. Lichao Wang and Dr. Jianzhong Shang for their contribution to the paper.

References

[1] Z. Nan, S. Sun, J. Wu, X. Meng, and G. Tao, "A real-time micro-sensor motion capture system," in *Advances in Wireless Sensor Networks*. Springer, 2013, pp. 685–694.

[2] X. Yun and E. Bachmann, "Design, implementation, and experimental results of a quaternion-based Kalman filter for human body motion tracking," *IEEE Transactions on Robotics*, vol. 22, no. 6, pp. 1216–1227, 2006.

[3] Z.-Q. Zhang, W.-C. Wong, and J.-K. Wu, "Ubiquitous human upper-limb motion estimation using wearable sensors," *Information Technology in Biomedicine, IEEE Transactions on*, vol. 15, no. 4, pp. 513–521, 2011.

[4] Z.-Q. Zhang, L.-Y. Ji, Z.-P. Huang, and J.-K. Wu, "Adaptive information fusion for human upper limb movement estimation," *Systems, Man and Cybernetics, Part A: Systems and Humans, IEEE Transactions on*, vol. 42, no. 5, pp. 1100–1108, 2012.

[5] P. Robertson, M. Angermann, and B. Krach, "Simultaneous localization and mapping for pedestrians using only foot-mounted inertial sensors," in *Proceedings of the 11th international conference on Ubiquitous computing*, 2009, pp. 93–96.

[6] M. J. Floor-Westerdijk, H. Schepers, P. H. Veltink, E. H. van Asseldonk, and J. H. Buurke, "Use of inertial sensors for ambulatory assessment of center-of-mass displacements during walking," *Biomedical Engineering, IEEE Transactions on*, vol. 59, no. 7, pp. 2080–2084, 2012.

[7] R. Rogers, *Applied mathematics in integrated navigation systems*. AIAA Education Series, 2003, vol. 1.

[8] A. Chatfield, *Fundamentals of high accuracy inertial navigation*. AIAA (American Institute of Aeronautics & Astronautics), 1997, vol. 174.

[9] A. Kim and M. Golnaraghi, "Initial calibration of an inertial measurement unit using an optical position tracking system," in *Position Location and Navigation Symposium, 2004. PLANS 2004.* IEEE, 2004, pp. 96–101.

[10] D. Marioli, E. Sardini, and A. Taroni, "computerized system for the very low frequency calibration of accelerometers," in *Proc. 6th Int. Symp. Intelligent Instrumentation for Remote and On-Site Measurements*, 1993, pp. 437–442.
[11] J. Lötters, J. Schipper, P. Veltink, W. Olthuis, and P. Bergveld, "Procedure for in-use calibration of triaxial accelerometers in medical applications," *Sensors and Actuators A: Physical*, vol. 68, no. 1-3, pp. 221–228, 1998.
[12] Z. Wu, Z. Wang, and Y. Ge, "Gravity based online calibration for monolithic triaxial accelerometers' gain and offset drift," in *Intelligent Control and Automation, 2002. Proceedings of the 4th World Congress on*, vol. 3, 2002, pp. 2171–2175.
[13] I. Skog and P. Händel, "Calibration of a mems inertial measurement unit," in *XVII IMEKO World Congress on Metrology for a Sustainable Development, September*. Citeseer, 2006, pp. 17–22.
[14] Z. Syed, P. Aggarwal, C. Goodall, X. Niu, and N. El-Sheimy, "A new multi-position calibration method for mems inertial navigation systems," *Measurement Science and Technology*, vol. 18, p. 1897, 2007.
[15] S. Shen, C. Chen, and H. Huang, "A new calibration method for mems inertial sensor module," in *Advanced Motion Control, 2010 11th IEEE International Workshop on*. IEEE, 2010, pp. 106–111.
[16] W. Li, Q. Du, and P. Mi, "A mems inertial sensor and amr magnetic sensor calibration method," in *Information, Communications and Signal Processing (ICICS) 2011 8th International Conference on*. IEEE, 2011, pp. 1–5.
[17] D. Gebre-Egziabher, G. H. Elkaim, J. David Powell, and B. W. Parkinson, "Calibration of strapdown magnetometers in magnetic field domain," *Journal of Aerospace Engineering*, vol. 19, no. 2, pp. 87–102, 2006.
[18] V. Renaudin, M. H. Afzal, and G. Lachapelle, "New method for magnetometers based orientation estimation," in *Position Location and Navigation Symposium (PLANS), 2010 IEEE/ION*. IEEE, 2010, pp. 348–356.
[19] J. Vasconcelos, G. Elkaim, C. Silvestre, P. Oliveira, and B. Cardeira, "Geometric approach to strapdown magnetometer calibration in sensor frame," *Aerospace and Electronic Systems, IEEE Transactions on*, vol. 47, no. 2, pp. 1293–1306, 2011.
[20] Z.-Q. Zhang, X.-L. Meng, and J.-K. Wu, "Quaternion-based kalman filter with vector selection for accurate orientation tracking," *Instrumentation and Measurement, IEEE Transactions on*, vol. 61, no. 10, pp. 2817–2824, 2012.
[21] S. Bonnet, C. Bassompierre, C. Godin, S. Lesecq, and A. Barraud, "Calibration methods for inertial and magnetic sensors," *Sensors and Actuators A: Physical*, vol. 156, no. 2, pp. 302–311, 2009.
[22] A. Fitzgibbon, M. Pilu, and R. Fisher, "Direct least square fitting of ellipses," *Pattern Analysis and Machine Intelligence, IEEE Transactions on*, vol. 21, no. 5, pp. 476–480, 1999.
[23] I. Markovsky, A. Kukush, and S. Huffel, "Consistent least squares fitting of ellipsoids," *Numerische Mathematik*, vol. 98, no. 1, pp. 177–194, 2004.
[24] Q. Li and J. G. Griffiths, "Least squares ellipsoid specific fitting," *Geometric Modeling and Processing*, vol. 0, p. 335, 2004.
[25] N. Chernov and H. Ma, "Least squares fitting of quadratic curves and surfaces," *Computer Vision*, pp. 285–302, 2011.
[26] B. Lo and G. Yang, "Key technical challenges and current implementations of body sensor network," in *Proc. 2nd International Workshop on Body Sensor Networks (BSN 2005)*, 2005.
[27] A. D. ADXL330, http://www.analog.com/en/sensors/inertial-sensors/adxl330/products/product.html.
[28] I. ITG-3200, http://invensense.com/mems/gyro/itg3200.html.
[29] H. HMC5843, www.magneticsensors.com/datasheets/HMC5843.pdf.
[30] BTSBioengineering, http://www.btsbioengineering.com/.

Targets Tracking.

Zhi-Qiang Zhang received the B.E. degree in computer science and technology from School of Electrical Information and Engineering, Tianjian University, China, in 2005, and the Ph.D. degree from the Sensor Network and Application Research Center, Graduate University, Chinese Academy of Sciences, Beijing, China, in 2010.
He is currently a Research Associate with the Hamlyn Centre for Robotic Surgery, Imperial College, London. His research interests include Body Sensor Network, Information Fusion, Machine Learning and

Guang-Zhong Yang (S'90-M'91-SM'08-F'11) Ph.D. degree in computer science from Imperial College London, London, U.K.
He is the Director, Co-Founder, and currently chairs the Hamlyn Centre for Robotic Surgery, Imperial College London. His main research interests include biomedical imaging, sensing, and robotics.
Dr. Yang is a Fellow of the Royal Academy of Engineering, the Institution of Engineering and Technology, and the American Institute for Medical Biological Engineering.